The underappreciated impact of emission source profiles on the simulation of $PM_{2.5}$ components: New evidence from sensitivity analysis

Zhongwei Luo[a,b,1], Yan Han[a,b,c,1], Kun Hua[a,b], Yufen Zhang[a,b*], Jianhui Wu[a,b], Xiaohui Bi[a,b], Qili Dai[a,b], Baoshuang Liu[a,b], Yang Chen[c], Xin Long[c], Yinchang Feng[a,b*]

[a]State Environmental Protection Key Laboratory of Urban Ambient Air Particulate Matter Pollution Prevention and Control & Tianjin Key Laboratory of Urban Transport Emission Research, College of Environmental Science and Engineering, Nankai University, Tianjin 300350, China.

[b]CMA-NKU Cooperative Laboratory for Atmospheric Environment-Health Research, Tianjin 300350, China.

[c]Research Center for Atmospheric Environment, Chongqing Institute of Green and Intelligent Technology, Chinese Academy of Sciences, Chongqing 400714, China.

*Corresponding authors:

Y. F. Zhang (zhafox@nankai.edu.cn). And Y. C. Feng (fengyc@nankai.edu.cn).

[1]Z. W. Luo and Y. Han equally contribute to this work

Abstract

The chemical transport model (CTM) is an essential tool for air quality prediction and management, widely used in air pollution control and health risk assessment. However, the current models do not perform very well in simulating $PM_{2.5}$ components. Studies suggested that the uncertainties of model chemical mechanism, source emission inventory and meteorological field can cause inaccurate simulation results. Still, the emission source profile of $PM_{2.5}$ has not been fully taken into account in current numerical simulation. This study aims to answer (1) Whether the variation of source profile adopted in ~~chemical transport models (~~CTMs~~)~~ has an impact on the simulation of $PM_{2.5}$ chemical components? (2) How much does it impact? (3) How does the impact work? Based on the characteristics and variation rules of chemical components in typical $PM_{2.5}$ sources, different simulation scenarios were designed and the sensitivity of components simulation results to $PM_{2.5}$ sources profile was explored. Our findings showed that the influence of source profile changes on simulated $PM_{2.5}$ concentration was insignificant, but its impact on $PM_{2.5}$ components could not be ignored. The variations of simulated components ranged from 8% to 167% under selected different source profiles, and simulation results of some components were sensitive to the adopted $PM_{2.5}$ source profile in CTMs. These influences are connected to the chemical mechanisms of the model since the variation of species allocations in emission sources directly affected the thermodynamic equilibrium system. We also found that the perturbation of the $PM_{2.5}$ source profile caused the variation of simulated gaseous pollutants, which indirectly indicated that the perturbation of the source profile affected the simulation of secondary $PM_{2.5}$ components. Given the vital role of air quality simulation in environment management and health risk assessment, the representativeness and timeliness of source profile should be considered.

Keywords

$PM_{2.5}$; source profile; component; numerical simulation; chemical transport model

1. Introduction

Ambient fine particulate matter ($PM_{2.5}$) pollution in some key regions of China has attracted much attention (Liang et al., 2020; Huang et al., 2021). The chemical components of $PM_{2.5}$, including elements (Al, Si, Fe, Mn, Ti, Cu, Zn, Pb, etc.), water-soluble ions (SO_4^{2-}, NO_3^-, Cl^-, F^-, NH_4^+, Na^+, K^+, Mg^{2+}, Ca^{2+}, etc.), and carbon-containing components (Organic Carbon, OC; Elemental Carbon, EC) (Yang et al., 2011; Li et al., 2013), have different physical and chemical properties, such as reactivity, thermal stability, particle size distribution, residence time, optical properties, health hazards, etc (Seinfeld and Pandis, 2006; Tang et al., 2006). According to long-term monitoring results, in most regions of China, SO_4^{2-}, NO_3^-, NH_4^+ and OC are the most important species in ambient $PM_{2.5}$ (Li et al., 2017a; Li et al., 2021), which has a certain adverse impact on human health (Shi et al., 2018) and ecosystem ~~(Han et al., 2019; Zhou et al., 2018)~~, such as acid rain in southwest China (Han et al., 2019), food security (Zhou et al., 2018), etc.

The chemical transport models (CTMs) play an important role in policy making for regulatory purposes. Based on the scientific understanding of atmospheric physical and chemical processes, CTMs are built to simulate the transport, reaction and removal of pollutants on a certain scale in horizontal and vertical directions. With the development of CTMs, the simulation accuracy of $PM_{2.5}$ concentration has been significantly improved. Higher requirements have been put forward for the precise simulation of $PM_{2.5}$ components so as to provide support for the use of CTMs in human health risk assessment, climate effects, pollution sources apportionment, and so on (Peterson et al., 2020; Lv et al., 2021). However, the current models perform not very well in simulating some components (for example, $PM_{2.5}$-bound sulfate, nitrate, ammonium, trace elements, etc.) (Zheng et al., 2015; Fu et al., 2016; Ying et al., 2018; Cao et al., 2021). In the current literature, the correlation coefficient (R) and normalized mean bias (NMB) are highly variable and inconsistent between the simulated and the observed values (listed in Table S1). This is mainly attributable to the uncertainties of

model chemical mechanism, source emission inventory and meteorological field simulation.

The chemical mechanisms involved in CTMs are derived from parameterized assumptions based on laboratory simulation and field observations. The actual atmospheric chemical processes are very complex, and some reaction mechanisms are still limitedly understood. In addition, the integration of chemical reactions and simplified treatment methods in the model cannot fully reflect the correlation among atmospheric pollutants. For example, in some model mechanisms, other important sulfate and nitrate formation pathways were added through new heterogeneous chemistry, including the chemical reaction between SO_2 and aerosol, $NO_2/NO_3/N_2O_3$ and aerosol (Zheng et al., 2015), nitrous acid oxidized SO_2 to produce sulfate (Zheng et al., 2020), dust particles promoted the oxidation of SO_2 (Yu et al., 2020), modified the uptake coefficients for heterogeneous oxidation of SO_2 to sulfate (Zhang et al., 2019), updated the heterogeneous N_2O_5 parameterization (Foley et al., 2010). Even though the aforementioned processes can significantly improve the simulation of SO_4^{2-} and NO_3^-, there is still a gap between the modeled and the actual atmospheric chemical processes.

The uncertainty of source emission inventory also significantly affects the simulation results of $PM_{2.5}$ components (Shi et al., 2017; Sha et al., 2019). Due to incomplete information or insufficient representativeness, pollutant emissions are sometimes overestimated or underestimated, and the method for temporal and spatial allocation also needs to be improved.

The uncertainty of meteorological field simulation is another crucial reason for the simulation deviation, especially on heavy pollution days, the variation trends of $PM_{2.5}$ chemical components were not well-captured (Ying et al., 2018; Qi et al., 2019; Wang et al., 2022). Precipitation is the key meteorological factor determining wet removal of pollutants; boundary layer height and wind speed are the main factors affecting convection and transport of pollutants; solar radiation, temperature and relative humidity are the key factors affecting the formation of secondary particles (Huang et

al., 2019; Chen et al., 2020). Some literature reported that deviation from precipitation and wind field simulation might lead to underestimation of SO_4^{2-}, NO_3^- and NH_4^+ (Cheng et al., 2015; Zhang et al., 2017). Devaluation of liquid water path and cloud cover cause a decrease of sulfate formation in cloud, and ultimately results in significantly underestimated components in simulation values (Sha et al., 2019; Foley et al., 2010). Underestimation of temperature and relative humidity may also cause adverse effects of temperature- and/or relative humidity-dependence chemical reaction in the simulation (Sha et al., 2019).

In particular, the emission source profile of $PM_{2.5}$ (Hereinafter referred to as "source profile"), creating speciated emission inventories for CTMs (Hsu et al., 2019), has not been fully taken into account in the current numerical simulation ~~by CTMs~~. In the reported literature, $PM_{2.5}$ species allocation coefficients of emission sources are commonly treated in the following ways: (1) allocated $PM_{2.5}$ components of source emissions by referring to source profile data in published literature or database like the US SPECIATE (Fu et al., 2013; Wang et al., 2014; Ying et al., 2018); (2) chemical profiles come from local measurement (Fu et al., 2013; Appel et al., 2013). However, with the development of production technology and the innovation of pollution treatment technology in recent years, some source profiles have changed dramatically (Bi et al., 2019), such as SO_4^{2-} from coal burning, SO_4^{2-} content in $PM_{2.5}$ is generally low in coal-fired power plant without desulfurizing facilities, while existing coal-fired power plants using limestone/gypsum wet desulphurization, the contents of SO_4^{2-} in $PM_{2.5}$ are significantly higher than that without desulfurization facilities (Zhang et al., 2020). The timeliness of $PM_{2.5}$ species allocation coefficients in current CTMs also needs to be considered.

This paper attempts to answer the following questions: (1) Whether the variation of the source profile adopted in the air quality model has an impact on the simulated results of $PM_{2.5}$ chemical components? (2) How much does it impact? (3) How does the impact work? Aiming at these problems above, chemical composition and its variation law for typical $PM_{2.5}$ emission sources are summarized, on this basis,

sensitivity tests are designed to identify whether $PM_{2.5}$ source profiles and species allocation in the model are important parameters that affect the simulation results of chemical components in $PM_{2.5}$. We take CMAQ (one of the most widely used CTMs), MEIC (a high-resolution inventory of anthropogenic air pollutants in China) as the carriers. The same kind of experiment is also applicable to other CTMs and emission inventories. The aim of this study is to provide support for the effective utilization of source profiles in the CTMs and improvement of the simulation schemes.

2. Model and Data

2.1 Model configuration

Weather Research and Forecasting model (WRF-3.7.1), the widely used Community Multiscale Air Quality model (CMAQv5.0.2), and Multi-resolution Emission Inventory for China (MEICv1.3) have been used in this study. MEIC provided the emission inventory which is developed by Tsinghua University, mainly tracked anthropogenic emissions in China including coal-fired power plants, industry, vehicles, residents and agriculture (http://meicmodel.org/?page_id=135) (Li et al., 2017b; Zheng et al., 2018). The WRF model was used to generate meteorological inputs for the CMAQ model. Three nested modeling domains consisting of 36 km×36 km (Dom1), 12 km×12km (Dom2), and 4 km×4km (Dom3) horizontal grid sizes were set, as shown in Fig. 1. The initial and boundary conditions for WRF were based on the North American Regional Reanalysis data archived at National Center for Atmospheric Research (NCAR). In addition, surface and upper air observations obtained from NCAR were used to further refine the analysis data. The major configurations we used in CMAQ were illuminated as follows: Gas-phase chemistry was based on the CB05 mechanism and the aerosol dynamics/chemistry was based on the aero6 module (cb05tucl_ae6_aq). The detailed model configurations were shown in Table S2, regional distribution of $PM_{2.5}$ emission sources were shown in Fig. S2.

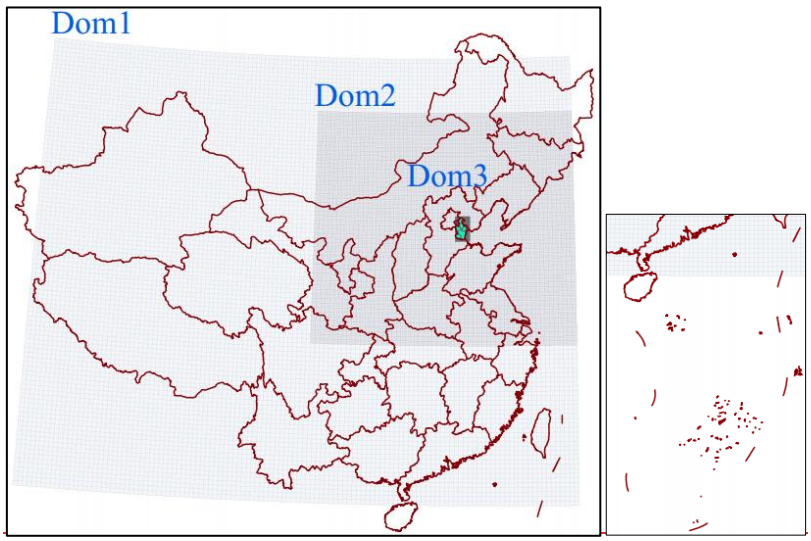

~~Fig.1 Modeling domains of the CMAQ model.~~

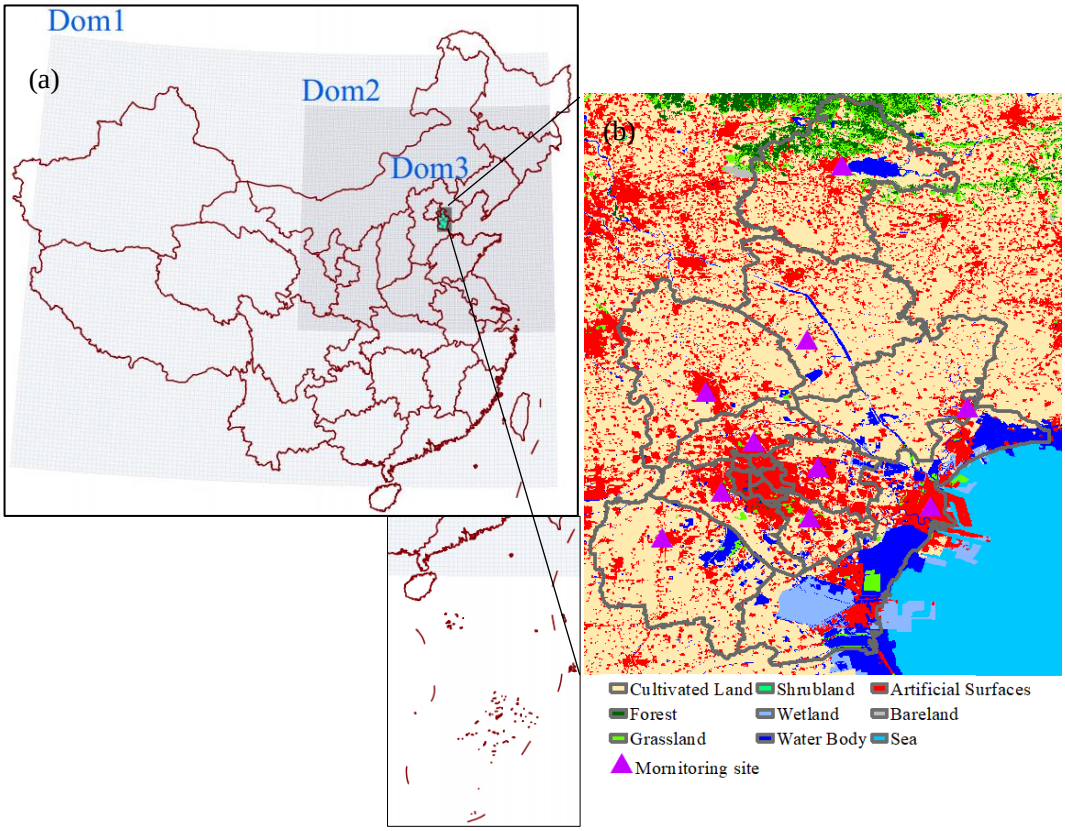

Fig.1 Modeling domains of the CMAQ model. (a) The three-domain nested CMAQ domains; (b) Land use and observation sites of Dom3 (Data source of Land use: GLOBELAND30, www.globeland30.org, National Geomatics Center of China).

2.2 Selection and comparison of $PM_{2.5}$ source profile

The $PM_{2.5}$ emission source profiles from database of Source Profiles of Air Pollution (SPAP) (http://www.nkspap.com:9091/), U.S. Environmental Protection Agency's (EPA) SPECIATE database (https://www.epa.gov/air-emissions-

modeling/speciate) as well as from published literature were selected, respectively. The SPAP was developed by the State Environment Protection Key Laboratory of Urban Particulate Air Pollution Prevention, Nankai University, China. This database contains more than 3000 size-resolved source profiles of stationary combustion sources, industrial processes, vehicle exhaust, biomass burning, dust and cooking emissions and other sources, collected from more than 40 cities in China since 2001. In addition to inorganic elements, water-soluble ions, OC, EC and other conventional components, some source profiles also encompass a series of tracer information, such as organic markers, isotopes, single particle mass spectrometry, VOCs and other gaseous precursors. Based on species in the aerosol chemical mechanism (AERO6) (Appel et al., 2013; Chapel Hill, 2012), we selected 15 components in $PM_{2.5}$ source profiles including Al, Ca, Cl, EC, Fe, K, Mg, Mn, Na, OC, Si, Ti, NH_4^+, NO_3^- and SO_4^{2-}, the remaining components are classified as "other". Emission sources are divided into four main categories referred to the classification in MEIC: coal combustion by power plants (PP), industrial processes (IN), residential emission (RE) and transportation sector (TR).

Coal-fired power plants remain the main coal consumers in China, which accounted for 50.2% of total coal consumption in 2019 (NBS, 2021) and gained much more attention (Wu et al., 2022), especially with the wide implementation of the strictest ultralow emission standards, $PM_{2.5}$ emission characteristics have changed accordingly (Wu et al., 2020). There are obvious differences in $PM_{2.5}$ source profiles between SPAPPC (SPAP database and published source profiles in China) and SPECIATE (SPECIATE database), detailed information is shown in Table S3. The percentages of species in PP source profiles are plotted in Fig. 2. The main components in SPAPPC are sorted by Si, SO_4^{2-}, OC, Ca with average values of 8.7±6.8%, 8.5±11.5%, 6.8±9.1% and 6.5±6.9%, respectively; The SPECIATE are enriched in SO_4^{2-} (16.9%±20.0%), OC (12.7±21.8%), Si (9.6±5.0%) and Ca (9.3±7.3%), higher than SPAPPC. Coal properties, burning conditions, pollution control measures and sampling methods are the main reasons for those great percentage fluctuations. Different treatment processes of flue gases, e.g. wet/dry limestone, ammonia and double-alkali

flue gas desulfurization, will affect the percentages of components in source profiles (Zhang et al., 2020). It has been reported that the percentage of Ca, Mg, SO_4^{2-} and Cl^- in PP profiles increased after the limestone-gypsum method was used in coal-fired power plants (Bi et al., 2019). Besides that, the percentage of Cl^- in SPAPPC is obviously higher than that in SPECIATE, which might attribute to the generally higher Cl^- content in raw coal in China (Guo et al., 2004).

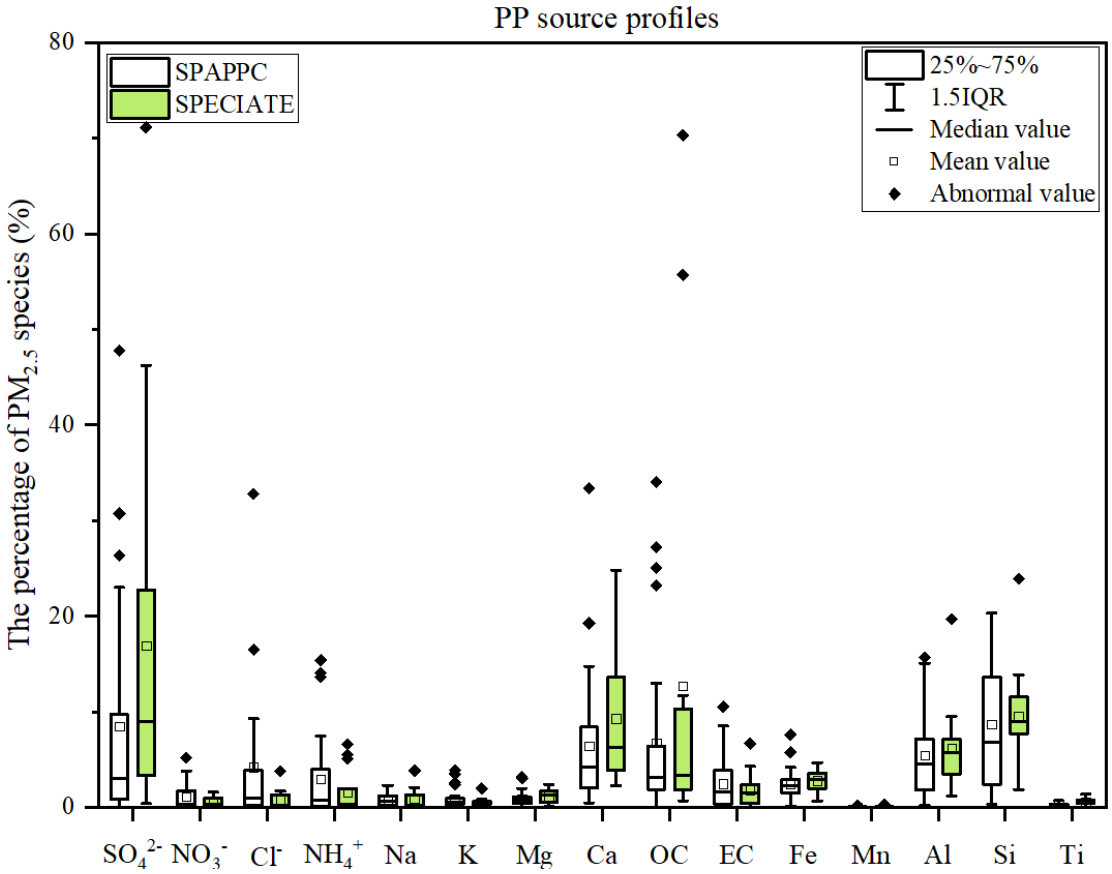

Fig. 2 Chemical profiles for $PM_{2.5}$ emitted from coal-fired power plant (PP). Data obtained from SPAPPC (SPAP database and published source profiles in China) and SPECIATE (U.S. EPA SPECIATE database)

Industrial emissions are one of the major sources of $PM_{2.5}$ (Hopke et al., 2020), the percentages of Ca, Fe, OC and SO_4^{2-} are relatively high both in SPAPPC and SPECIATE of industrial processes, but the shares in different source profile database varied (Detailed information were shown in Table S4~S7). In SPAPPC, these four components account for 16.4±14.9%, 10.4±14.4%, 6.9±6.1%, 6.2±6.4%, the proportions in SPECIATE are 10.4±9.8%, 11.4±10.6%, 8.5±4.9%, 16.3±13.3%, respectively (Fig. 3). Large variations of components and their percentages in industrial

processes are attributed to the manufacturing processes, raw material, pollution control measures and so on (Ji et al., 2017; Bi et al., 2019; Gao et al., 2022). For example, Ca, Al, OC and SO_4^{2-} are found to have the highest percentage in cement sources (Guo et al., 2021); Fe, Si and SO_4^{2-} are the most abundant species in steel industry emission (Guo et al., 2017).

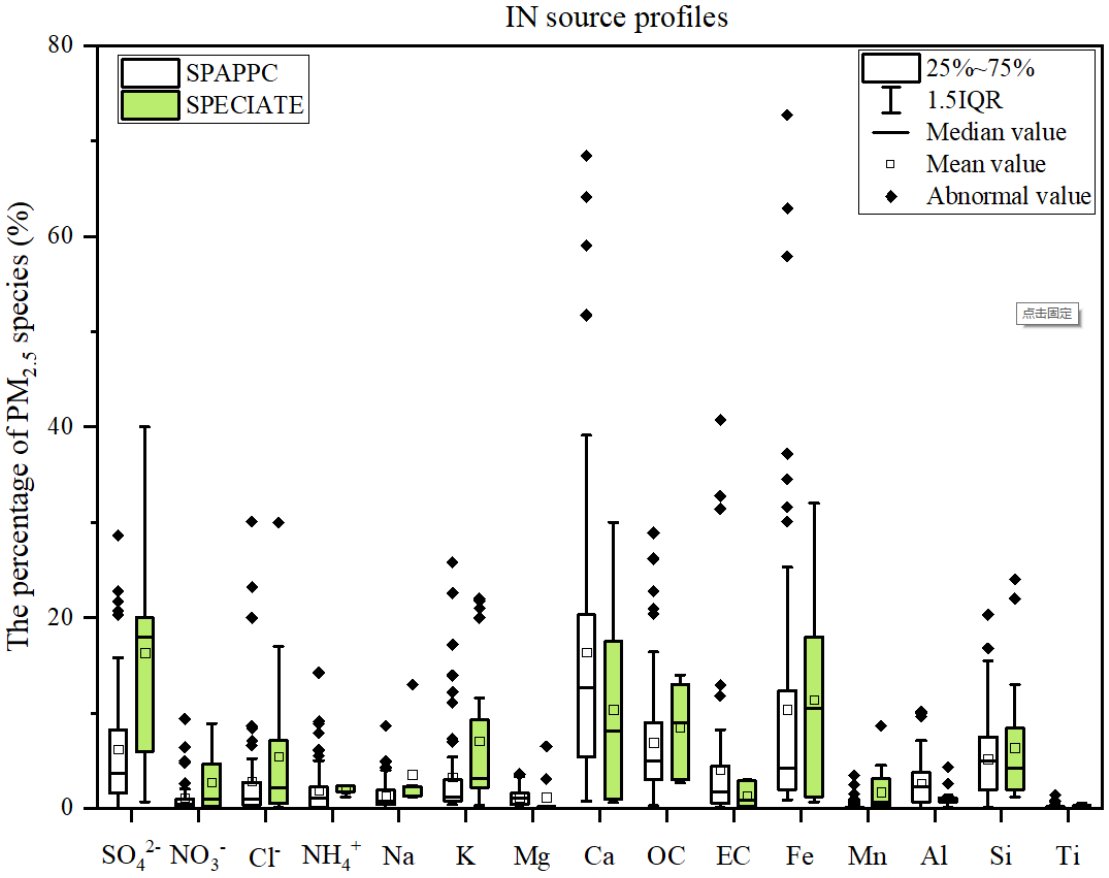

Fig. 3 Chemical profiles for $PM_{2.5}$ emitted from industry processes (IN). Data obtained from SPAPPC (SPAP database and published source profiles in China) and SPECIATE (U.S. EPA SPECIATE database)

Traffic contributed a large fraction of $PM_{2.5}$ in many locations (Hopke et al., 2022). It is well-known that the transportation sector makes a dominant contribution of OC and EC. The main components of $PM_{2.5}$ emitted from traffic sources are OC, EC and SO_4^{2-} both in SPAPPC and SPECIATE, but still vary in wide range (Detailed information was given in Table S8~S10). In SPAPPC, the percentages of OC, EC and SO_4^{2-} are 40.8±15.0%, 23.1±13.8%, 3.1±3.7%, and in SPECIATE, the percentages are 40.6±16.4%, 36.1±21.5%, 6.4±9.9%, respectively (Fig. 4). These significant differences mainly attribute to the vehicle type, fuel quality, mixing ratio between oil

and gas and the combustion phase in vehicle engine and so on (Xia et al., 2017).

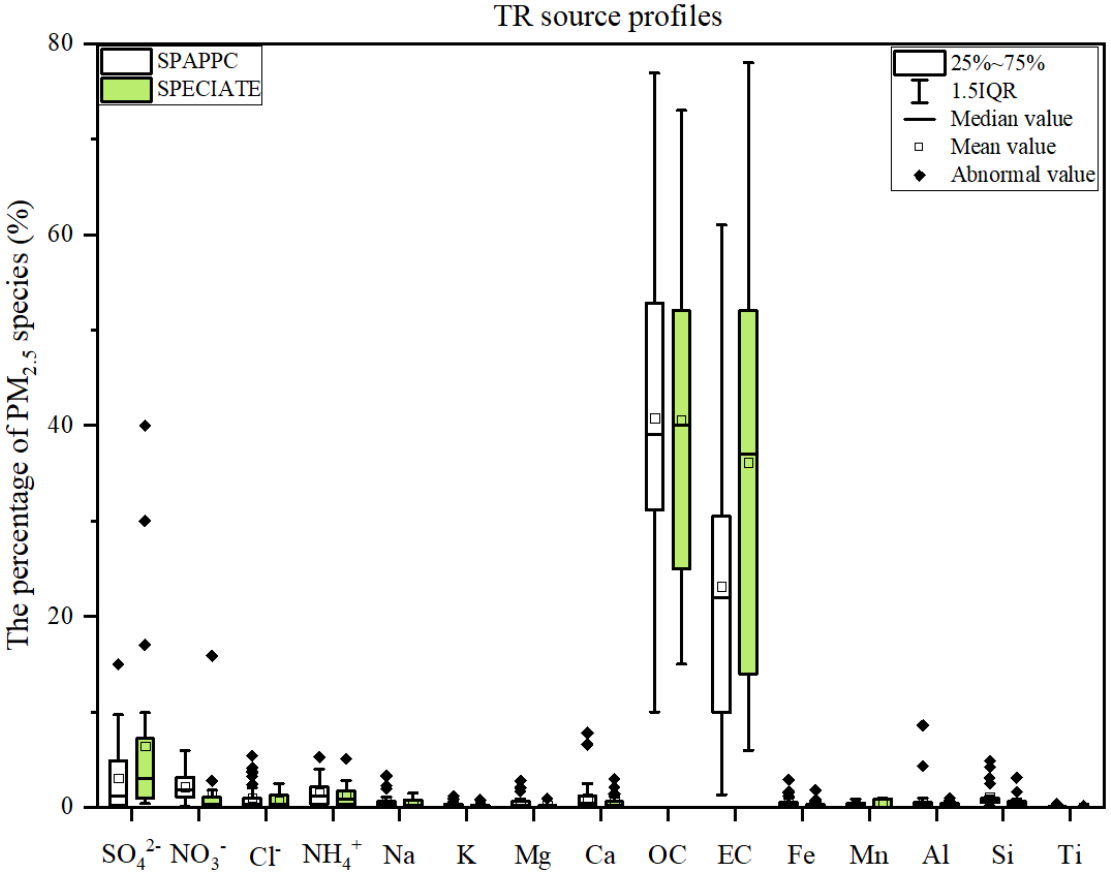

Fig. 4 Chemical profiles for $PM_{2.5}$ emitted from transportation sector (TR). Data obtained from SPAPPC (SPAP database and published source profiles in China) and SPECIATE (U.S. EPA SPECIATE database)

Residential coal combustion, as the leading source of global $PM_{2.5}$ emission (Weagle et al., 2018), has a much higher emission factor than coal-fired power plant (Wu et al., 2022). The fraction of components varied greatly in the profiles measured from SPAPPC and SPECIATE (Detailed information was given in Table S11), SO_4^{2-}, OC, NH_4^+ and EC make the main contribution to $PM_{2.5}$ emitted from residential coal combustion. In SPAPPC, the average percentages of SO_4^{2-}, OC, NH_4^+, EC are 27.1±10.1%, 20.7±20.6%, 11.3±7.7%, 2.6±2.8%, respectively. In SPECIATE, the average percentages are OC (58.2±14.0%), EC (24.6±5.4%), SO_4^{2-} (3.2±2.3%) and NH_4^+ (1.6±1.0%) (Fig. 5). Total percentages of OC and EC in SPECIATE are over 80%, obviously higher than that in SPAPPC, while a higher percentage of SO_4^{2-}, Cl^-, K and Si are observed in SPAPPC. The coal type and properties, burning condition are the main factors affecting the percentages of $PM_{2.5}$ components, like the chunk coal burning

has relatively higher percentages of OC, EC, SO_4^{2-}, NO_3^- and NH_4^+ than honeycomb briquette (Wu et al., 2021; Song et al., 2021).

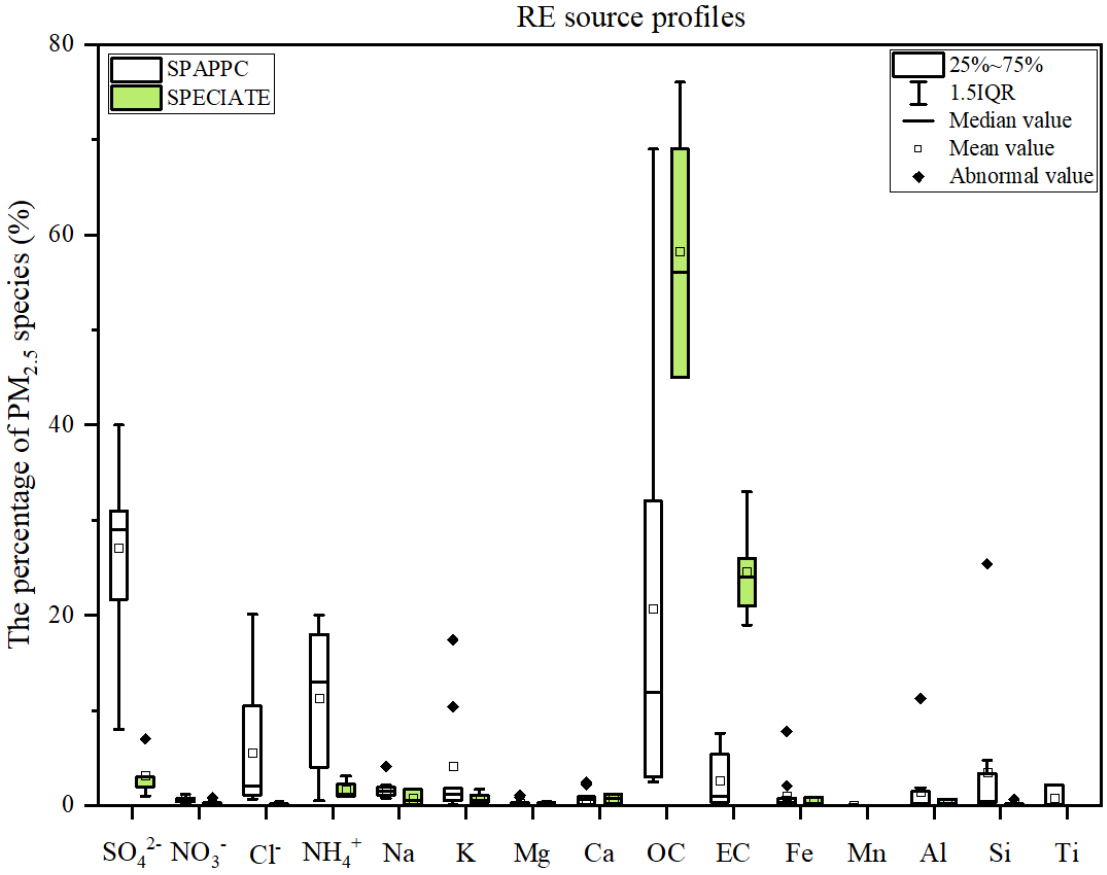

Fig. 5 Chemical profiles for $PM_{2.5}$ emitted from residential coal combustion (RE). Data obtained from SPAPPC (SPAP database and published source profiles in China) and SPECIATE (U.S. EPA SPECIATE database)

Briefly, many factors can affect $PM_{2.5}$ source profiles, and with the innovation of manufacturing technique and pollution control technology, changes in fuel and raw and auxiliary materials, the main chemical components and their percentages would change dramatically. To explore whether the variations of source profile would be one of the important factors affecting the simulation results of $PM_{2.5}$ species in CTMs, we designed a series of simulation tests as follows.

3 Whether the variation of source profile adopted in CTMs has an impact on the simulation of chemical components in $PM_{2.5}$?

In this part, we separately selected source profiles from SPAPPC and SPECIATE databases and applied them in emission inventory for simulating $PM_{2.5}$ and its

components with other modeling conditions unchanged, corresponding to case CMAQ_SPA and CMAQ_SPE. The detailed information ~~on~~ of source profiles is shown in Figure S1. To determine the similarity between the two groups of source profiles, Coefficient ~~divergence~~ Divergence (CD) is calculated using the following formula (Wongphatarakul et al., 1998):

$$CD_{jk} = \sqrt{\frac{1}{p}\sum_{i=1}^{p}\left(\frac{x_{ij}-x_{ik}}{x_{ij}+x_{ik}}\right)^2} \quad \text{..... (1)}$$

Where CD_{jk} is the coefficient of divergence of source profile j and k, p was the number of chemical components in source profile, x_{ij} is the weight percentage for chemical component i in source profile j, x_{ik} is the weight percentage for i in source profile k (%). The CD value is in the range of 0 to 1, if the two source profiles are similar, the value of CD is close to 0; if the two are very different, the value was close to 1.

By comparing the selected SPAPPC source profiles with the selected SPECIATE source profiles, the coefficient divergences for the four main source categories were $CD_{PP}(0.67)>CD_{RE}(0.62)>CD_{TR}(0.60)>CD_{IN}(0.60)$, which meant the selected source profiles in the two simulation cases were quite different. The simulated concentration of $PM_{2.5}$ and its components (For this part and each test case in next section) at 10 ambient air quality monitoring stations (Table S12) were extracted from CMAQ outputs of the innermost simulation domain. We selected one air quality monitoring station to study the influence of $PM_{2.5}$ source profile on numerical simulation of $PM_{2.5}$-bound components and to explore the relevant laws in the atmosphere, then used the left 9 sites to further illustrate the conclusions suggested.

The simulation results for $PM_{2.5}$ species under CMAQ_SPA and CMAQ_SPE cases also showed big differences (as shown in Fig. 6 and Table S13), in which the largest difference in simulated concentration was EC with CAMQ_SPE giving higher by 167% than CMAQ_SPA; For OC and Mn, higher values were also given by CMAQ_SPE than by CMAQ_SPA (45% and 126% on average, respectively); For the remaining components, the simulated concentration by CMAQ_SPE was lower than

CMAQ_SPA with Ti (58%), Na (55%), Mg (53%), Ca (51%), Al (33%), Cl (30%), K (29%), Si (22%), Fe (16%), NH_4^+ (9%), SO_4^{2-} (9%), NO_3^- (8%), separately. While the simulated $PM_{2.5}$ concentrations under the two cases were quite close. The influence of source profile variation on the simulated $PM_{2.5}$ concentration was not significant, but the influence on the simulation of chemical components in $PM_{2.5}$ could not be ignored.

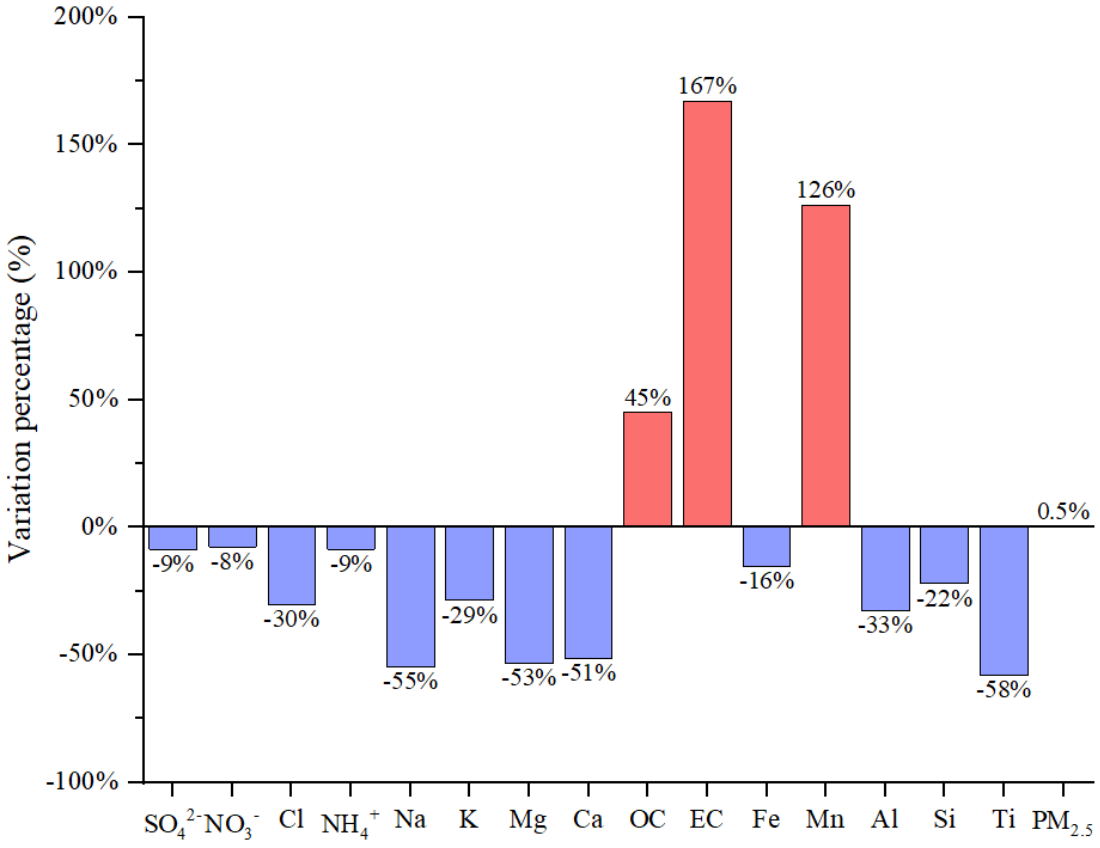

Fig. 6 The percentage difference of simulated concentration ($PM_{2.5}$ and its components) between CMAQ_SPE and CAMQ_SPA (relative to CAMQ_SPA); $PM_{2.5}$ source profiles from SPAPPC and SPECIATE database were applied in emission inventory for simulating $PM_{2.5}$ and its components, corresponding to case CMAQ_SPA and CMAQ_SPE, respectively.

4 How much did the variation of source profile adopted in CTMs impact on the simulation of chemical components in $PM_{2.5}$?

In order to quantitatively characterize how much the source profiles affect the simulation results of $PM_{2.5}$ and its components, we selected the chemical composition of code 000002.5 (Variety of different categories, used for the overall average

composite profiles (Hsu et al., 2019)) in the US EPA Speciate_5.0_0 database as species allocation of $PM_{2.5}$ components. The corresponding percentages of EC, OC, Mn, Fe, Ti, Al, Si, Ca, Mg, K, Na, Cl, NH_4^+, NO_3^- and SO_4^{2-} in $PM_{2.5}$ were shown in Fig. 7 (SGL, base case simulation).

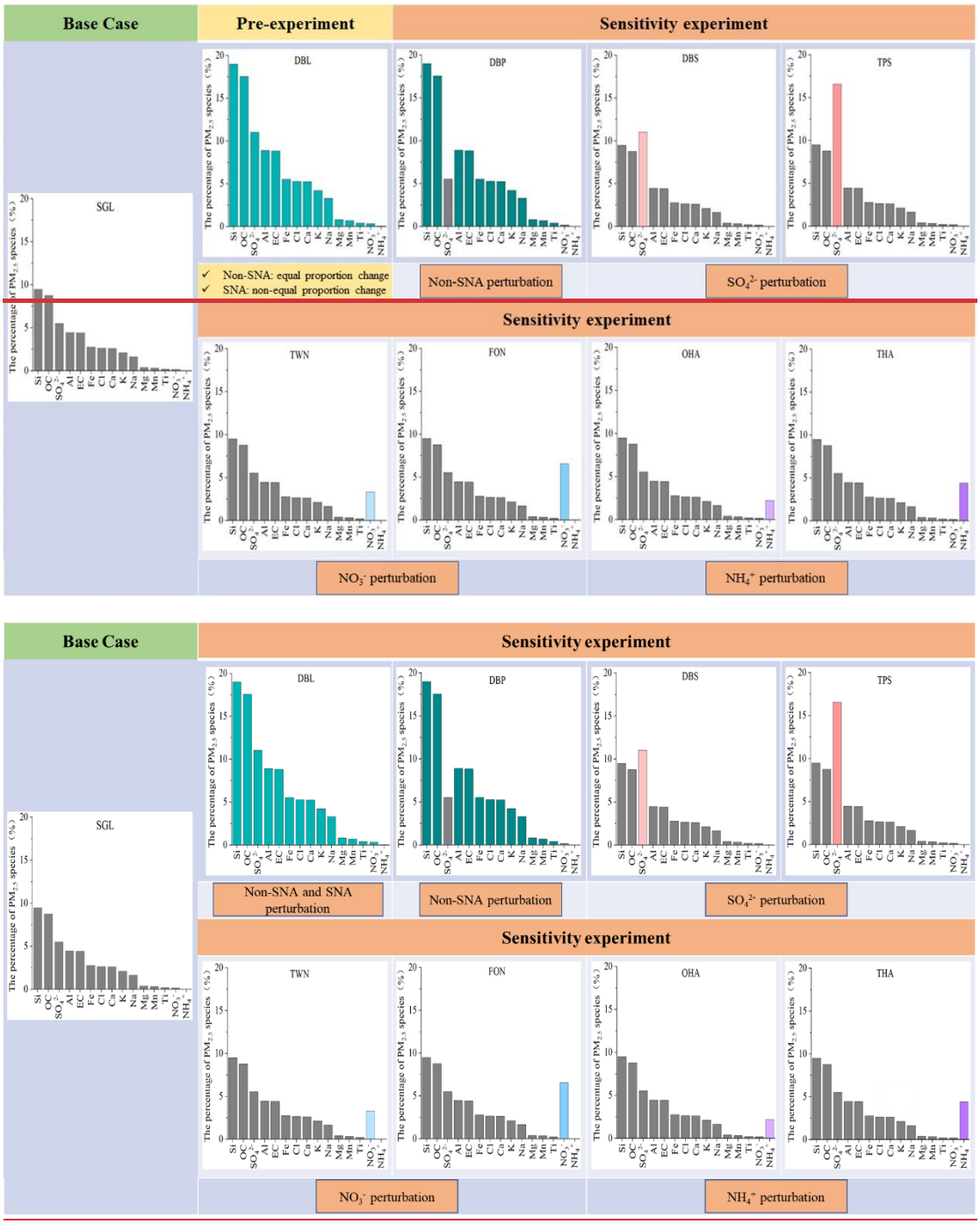

Fig. 7 The general roadmap of sensitivity tests
(The histogram in each case were the speciation profile in CTMs)

Table 1 The content of sensitivity experiment cases

Cases	Description
~~Pre-experiment~~cCase S0 (DBL): add perturbation to Non-SNA and SNA	The percentage of all the listed components in the source profile of base case (SGL) were doubled, and the proportion of unlisted components (Other) decreased to 9%.
Case S1 (DBP): add perturbation to Non-SNA	The percentages of non-SNA were doubled and SNA(SO_4^{2-}, NO_3^-, NH_4^+) species stayed the same with that in SGL (the cumulative percentage of listed species was 85.3%), the proportion of unlisted components decreased to 14.7%.
Case S2 (DBS and TPS): add perturbation to SO_4^{2-}	The percentage of SO_4^{2-} was doubled (11%, DBS, represented Double Sulfate), tripled (16.5%, TPS, represented Triple Sulfate) and the other listed 14 species stayed the same with that in SGL (the cumulative percentage of listed species was 51% and 57%, respectively), the proportion of unlisted components decreased to 49% and 43%.
Case S3 (TWN and FON): add perturbation to NO_3^-	The NO_3^- content was raised up to 20 times (3.3%, TWN) and 40 times (6.6%, FON) of that in SGL (0.16%), the other 14 species stayed the same with SGL (the cumulative percentage of listed species was 48.6% and 51.9%, respectively), the proportion of unlisted components decreased to 51.4% and 48.1%.
Case S4 (OHA and THA): add perturbation to NH_4^+	The NH_4^+ content was raised up to 100 times (2.2%, OHA), 200 times (4.4%, THA) of that in SGL (0.02%), the other 14 species stayed the same with SGL (the cumulative percentage of listed species was 47.7% and 49.9%, respectively), the proportion of unlisted components decreased to 52.3% and 50.1%.

Note: The source profiles in all cases listed in the table were calculated based on the base case SGL. In the design of simulation cases, the reason why the disturbance amplitude of NH_4^+ and NO_3^- were significantly higher than that of other components such as SO_4^{2-} and Non-SNA, was because the percentages of NH_4^+ and NO_3^- in the base source profile (SGL, based on the chemical composition of code 000002.5 in the EPA Speciate_5.0_0 database) were very low, while the percentage of NH_4^+ and NO_3^- in SPAPPC exhibited in section 2.2 were orders of magnitude higher than those in SGL.

316 Given the large number and complex chemical composition of $PM_{2.5}$, it is
317 advisable to classify it reasonably before designing sensitivity experiments. The ~~pre-~~
318 ~~experiment~~Case S0 was to double the percentage of the listed 15 components mentioned
319 above (SGL) in $PM_{2.5}$ species allocation for emission sources (DBL case, the
320 cumulative percentage was 91%, the details were shown in Fig. 7 and Table 1). As the
321 percentage of these components increased, the proportion of unlisted components

(represented by Other) decreased to 9% in order to meet the requirement that the total percentage of all components is 100%. Then we compared the simulation results before (SGL case) and after perturbation (DBL case) in species allocation of $PM_{2.5}$ sources.

In the case DBL, when the percentage of all the components except "other" were doubled in the source profile, the simulated concentrations of Al, Ca, Cl, EC, Fe, K, Mg, Mn, Na, OC, Si and Ti doubled as well, while the simulated concentration of NO_3^-, SO_4^{2-} and NH_4^+ only increased at about 3%, 10% and 4%, respectively, although the simulated concentration of $PM_{2.5}$ was not obviously changed (Detailed simulation results were shown in Table S14). Through this ~~pre-experiment~~Case S0, we found that the results for SNA (SO_4^{2-}, NO_3^-, and NH_4^+) and Non-SNA were obviously different. Therefore, we divided the components in the source profile into two groups (Non-SNA and SNA) and designed a series of sensitivity tests listed in next section to further explore how species allocation of $PM_{2.5}$ in emission sources of CTMs would affect the simulation results.

4.1 Sensitivity tests design

Based on the ~~pre-experiment~~Case S0 results, sensitivity tests were designed by changing the percentages of the target components and related components in the base case (SGL): perturbation on each component of Non-SNA, perturbation on SO_4^{2-}, perturbation on NO_3^-, and perturbation on NH_4^+. The general roadmap of sensitivity tests was shown in Fig. 7, and the illustration of each case was summarized in Table 1. The basic rules must be followed: a) perturbation on the percentage of each component in source profile fell within the variation range of its measured value described in section 2.2. b) The sum of the percentage of listed Non-SNA, SNA and Other components in $PM_{2.5}$ source profile was 100%.

4.2 Evaluation index for simulation result

In order to quantify the concentration changes of simulated $PM_{2.5}$ components caused by the perturbation in source profile, we proposed the sensitivity coefficient (δ) as evaluation index. The calculation formula is as follows:

$$\delta_i = \begin{cases} \dfrac{\dfrac{C_{i\_case}}{C_{PM_{2.5}\_case}} \times 100\% - \dfrac{C_{i\_base}}{C_{PM_{2.5}\_base}} \times 100\%}{P_{i\_case} - P_{i\_base}} & (For\ DBL\ and\ DBP) \\ \dfrac{\dfrac{C_{i\_case}}{C_{PM_{2.5}\_case}} \times 100\% - \dfrac{C_{i\_base}}{C_{PM_{2.5}\_base}} \times 100\%}{P_{j\_case} - P_{j\_base}} & (For\ other\ cases) \end{cases} \quad \cdots\cdots\cdots (2)$$

Wherein, δ_i is the sensitivity coefficient of component *i*, representing the change of the simulated value of its content in ambient $PM_{2.5}$ corresponded to 1% perturbation in the source profiles. C_{i_case} is the simulation result of component *i* in different sensitivity experiment cases, μg/m^3; C_{i_base} is the simulation result of components *i* in base case, μg/m^3; $C_{PM_{2.5}\_case}$ is the simulation result of $PM_{2.5}$ in different sensitivity experiment cases, μg/m^3; $C_{PM_{2.5}\_base}$ is the simulation result of $PM_{2.5}$ in base case, μg/m^3; P_{i_case} is the percentage of component *i* in different source profile of sensitivity experiment cases, %; P_{j_case} is the percentage of perturbed component *j* in different source profile of sensitivity experiment cases, %; P_{i_base} is the percentage of component *i* in base case source profile, %; ; P_{j_base} is the percentage of perturbed component *j* in base case source profile, %.

The positive value of δ means the simulated concentration of $PM_{2.5}$ component increases (decreases) with the increase (decrease) of the perturbation to the percentage of components in source profile, while the meaning of negative δ is just the opposite. If the absolute value of δ is less than or equal to 0.1, the simulated result of $PM_{2.5}$ chemical component is considered to be insensitive to the corresponding variation of source profile; If the absolute value of δ falls between 0.1 and 0.4 (included), the simulated results of $PM_{2.5}$ chemical component is considered to be sensitive to the variation of source profile; If the absolute value of δ is larger than 0.4, the simulated results of $PM_{2.5}$ chemical component is very sensitive to the variation of source profile. The greater the absolute value of δ is, indicates the variation of source profile adopted in CMAQ has more obvious impact on the simulated results of $PM_{2.5}$ chemical components.

4.3 The response of simulated $PM_{2.5}$ components

Fig.8 listed the sensitivity coefficients of simulated ambient $PM_{2.5}$ components to the perturbation of source profile under each test case. In case DBL (The percentage of all the listed components in the source profile of base case (SGL) was doubled), the sensitivity coefficient (δ) of NH_4^+ was negative, and the absolute value was the highest, indicating that the simulated proportion of NH_4^+ in ambient $PM_{2.5}$ decreased, and it was very sensitive to the variation of source profile. Conversely, the sensitivity coefficient of NO_3^- was close to 1, which illustrated that the simulated proportion of NO_3^- in ambient $PM_{2.5}$ increased proportionally with the change in source profile. The δ of SO_4^{2-} also showed a very sensitive property. The simulated Non-SNA concentrations were doubled when compared to the base case (SGL).

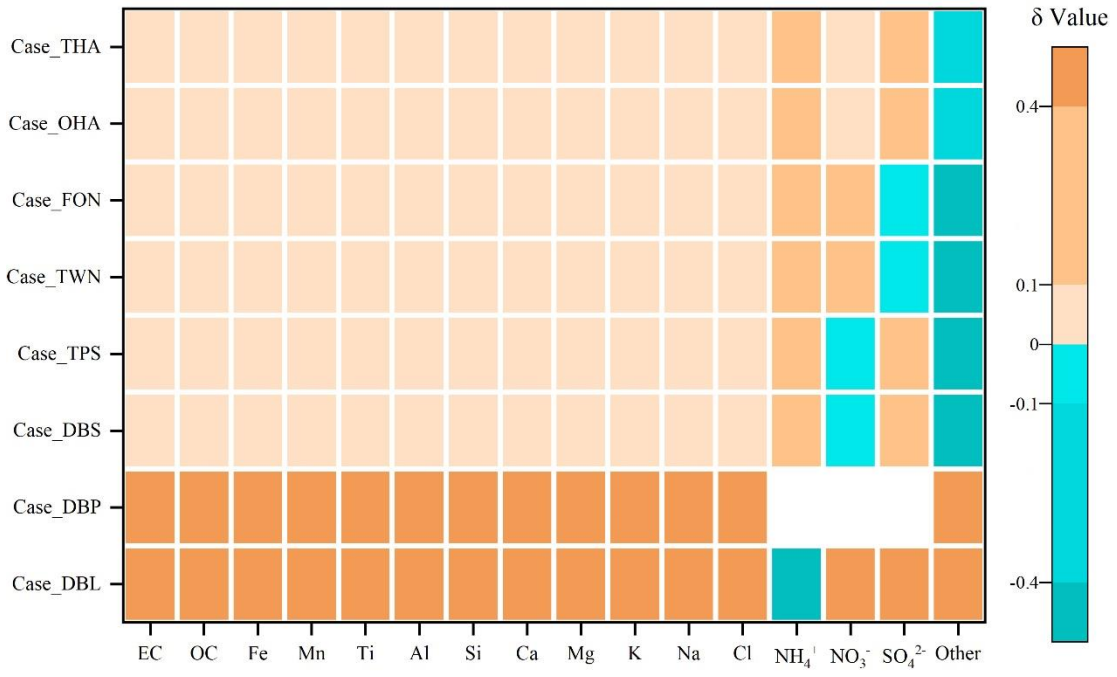

Fig. 8 The sensitivity coefficients (δ) of simulated components to the perturbation of adopted source profile in different cases. Note: Each small color box in the figure represented the sensitivity level (indicated by the legend on the right) of $PM_{2.5}$ components (the x-coordinate) in different cases (y-coordinate). The blank grids in DBP case indicated no perturbation to SNA in $PM_{2.5}$ source profile under this case.

In case DBP, when the percentages of listed Non-SNA in the source profile were doubled, the simulated proportions of Non-SNA (Al, Ca, Cl, EC, Fe, K, Mg, Mn, Na, OC, Si and Ti) in ambient $PM_{2.5}$ synchronous increased, and were very sensitive to the

change in the adopted source profile with a sensitivity coefficient (δ) of 0.5. Interestingly, the simulated concentration of SNA in ambient $PM_{2.5}$ also changed although the SNA in source profile did not change, the concentration of NO_3^- and SO_4^{2-} increased by 2% and 3%, respectively, NH_4^+ decreased by 10% (Detail simulation results of different cases were shown on Table S15~S21).

Under SO_4^{2-} perturbation cases (Case DBS and Case TPS), we found the simulated results of Non-SNA and NO_3^- had no obvious variation when compared with the base case. Either in Case DBS or in Case TPS, the δ of Non-SNA and NO_3^- were always between -0.1 to 0.1. But when the percentage of SO_4^{2-} was doubled in $PM_{2.5}$ source profile (DBS), the simulated concentration of NH_4^+ and SO_4^{2-} increased by 6% and 8%, respectively. In Case TPS (the percentage of SO_4^{2-} was tripled), the simulated concentration of NH_4^+ and SO_4^{2-} were increased by 11% and 16%, respectively. The δ of NH_4^+ and SO_4^{2-} were 0.12 and 0.36, sensitive toward to positive direction with the increase of SO_4^{2-} in the source profile.

In the situation of NO_3^- perturbation (Case TWN and Case FON), the simulated concentrations of Non-SNA hardly change when compared to the base case, while the changing characteristics of SNA concentrations were different. In cases TWN and FON, the simulation concentration of NH_4^+ increased by 2.6% and 5.4% when compared with the base case, the simulated NO_3^- increased by 14% and 30%, the simulated SO_4^{2-} decreased slightly, even could be neglected in some observation sites. The simulated concentrations of Non-SNA and SO_4^{2-} were insensitive to the perturbation of NO_3^- in $PM_{2.5}$ source profile; NH_4^+ was sensitive, and NO_3^- was very sensitive.

When we put perturbation to NH_4^+ in the source profile (Case OHA and Case THA), the simulation results of Non-SNA were almost not changed, the simulated concentration of SO_4^{2-}, NH_4^+, NO_3^- increased in OHA and THA. The δ of SNA to the variation of NH_4^+ in the source profile were positive and $\delta(SO_4^{2-}) > \delta(NH_4^+) > \delta(NO_3^-)$, SO_4^{2-} and NH_4^+ were sensitive to the NH_4^+ perturbation in the source profile, but NO_3^- was not so sensitive.

In general, the simulation results of components in ambient $PM_{2.5}$ were affected in

one way or another by the change of source profiles adopted by CMAQ. Both of the simulated Non-SNA and SNA were very sensitive to the perturbation of Non-SNA in source profile. When the percentage of SNA changed in the source profile, simulated concentrations of Non-SNA generally have little change, but the simulation results of SNA could change in different levels: the simulated SO_4^{2-} was very sensitive and NH_4^+ was sensitive to the perturbation of SO_4^{2-} in source profile, simulated NO_3^- was very sensitive and NH_4^+ was sensitive to the perturbation of NO_3^-, SO_4^{2-} and NH_4^+ were sensitive to the perturbation of NH_4^+. The simulated component such as SO_4^{2-} was influenced not only by the change of SO_4^{2-} itself but also by other components like some Non-SNA and NH_4^+ in the source profile. In other words, there was a linkage effect, variation of some components in the source profile would bring changes to the simulated results of other components.

5 How the variation of source profile adopted in CTMs impact on the simulation of chemical components in $PM_{2.5}$?

The variation of species allocation in emission sources directly affected the composition of aerosol system in CTMs. In CMAQv5.0.2, the aerosol thermodynamic equilibrium process was carried out according to ISORROPIA II, including a SO_4^{2-}-NO_3^--Cl^--NH_4^+-Na^+-K^+-Mg^{2+}-Ca^{2+}-H_2O system which was established on the basis of ISORROPIA I by adding the effects of K^+, Ca^{2+} and Mg^{2+} (Detailed equilibrium relations were shown in Table S22). Some assumptions had been made in the ISORROPIA model to simplify the simulation system (Fountoukis and Nenes, 2007): (1) Because the vapor pressure of sulfuric acid and metal salts (such as Na^+, Ca^{2+}, K^+, Mg^{2+}) were very low, it was assumed that all the sulfuric acid and metal salts in the system existed in the aerosol phase; (2) For ammonia in the system, it was preferred to have an irreversible reaction with sulfuric acid to produce ammonium sulfate. Only when there was still surplus NH_3 after the neutralization of H_2SO_4, can it have a reversible reaction with HNO_3 and HCl to produce NH_4NO_3 and NH_4Cl. (3) For sulfuric acid in the system, if there were metal ions (such as Ca^{2+}, Mg^{2+}, K^+, Na^+) in the system, sulfuric acid would react with metal ions to produce metal salts. Only in the case of

insufficient sodium, sulfuric acid would react with ammonia. Based on these assumptions, the ISORROPIA model introduced the following three judgment parameters (R_1, R_2 and R_3 were calculated by the following formulas) to determine the simulation subsystems. In this paper, R_1, R_2, R_3 and the corresponding solid phase species under different perturbation cases on source profiles were shown in Table 3. These components achieved thermodynamic equilibrium in the order of preference for more stable salts, obviously, the simulation processes of these components may influence each other.

$$R_1 = \frac{\left[NH_4^+\right]+\left[Ca^{2+}\right]+\left[K^+\right]+\left[Mg^{2+}\right]+\left[Na^+\right]}{\left[SO_4^{2-}\right]} \quad \text{(3)}$$

$$R_2 = \frac{\left[Ca^{2+}\right]+\left[K^+\right]+\left[Mg^{2+}\right]+\left[Na^+\right]}{\left[SO_4^{2-}\right]} \quad \text{(4)}$$

$$R_3 = \frac{\left[Ca^{2+}\right]+\left[K^+\right]+\left[Mg^{2+}\right]}{\left[SO_4^{2-}\right]} \quad \text{(5)}$$

Table 2 Potential aerosol species in ISORROPIA II under different cases

Cases	R_1	R_2	R_3	Solid phase species*
SGL、DBL TWN、FON	2.53	2.52	1.9	$CaSO_4$, $MgSO_4$, K_2SO_4, Na_2SO_4, NaCl, $NaNO_3$, NH_4Cl, NH_4NO_3
DBS	1.26	1.26	0.95	$CaSO_4$, $MgSO_4$, K_2SO_4, $KHSO_4$, Na_2SO_4, $NaHSO_4$, $(NH_4)_2SO_4$, NH_4HSO_4, $(NH_4)_3H(SO_4)_2$
TPS	0.84	0.84	0.63	$CaSO_4$, $KHSO_4$, $NaHSO_4$, NH_4HSO_4
DBP	5.04	5.03	3.79	$CaSO_4$, $MgSO_4$, K_2SO_4, $CaCl_2$, $Ca(NO_3)_2$, $MgCl_2$,
OHA	3.58	2.52	2.95	$Mg(NO_3)_2$, KCl, KNO_3, NaCl, $NaNO_3$, NH_4Cl,
THA	4.64	2.52	4.02	NH_4NO_3

* The solid phase species were determined based on the research of (Fountoukis and Nenes, 2007)

In Non-SNA perturbation case, when the percentage of Non-SNA in source profile doubled (Case DBP), meant there were more Na, K, Mg, Ca, Cl participated in aerosol chemistry, the model system needed more SO_4^{2-} and NO_3^- on the basis of charge balance and the thermodynamic equilibrium shifted to the direction of consuming Ca Mg, K and Na, which resulted in the increase of the simulated concentration of SO_4^{2-} and NO_3^-. Meanwhile, according to the rule of anions preferentially binding with nonvolatile cations in ISORROPIA, the increased cations Na^+, K^+, Mg^{2+}, Ca^{2+} directly leaded to

the decrease of anions binding with NH_4^+, there were less reaction dose between SO_4^{2-} and NH_4^+ to form $(NH_4)_2SO_4$ or NH_4HSO_4, ultimately resulted in a decrease in simulated concentration of NH_4^+ when compared to the base case. Because in this case more anions such as SO_4^{2-} were passively needed, according to the principle of chemical equilibrium mentioned above, the chemical conversion of SO_2 to SO_4^{2-} was promoted, the simulated secondary SO_4^{2-} increased, this could be proved by that the δ of SO_2 in Case DBP was negative (shown in Fig. 9, details of other monitoring stations were shown Table S24).

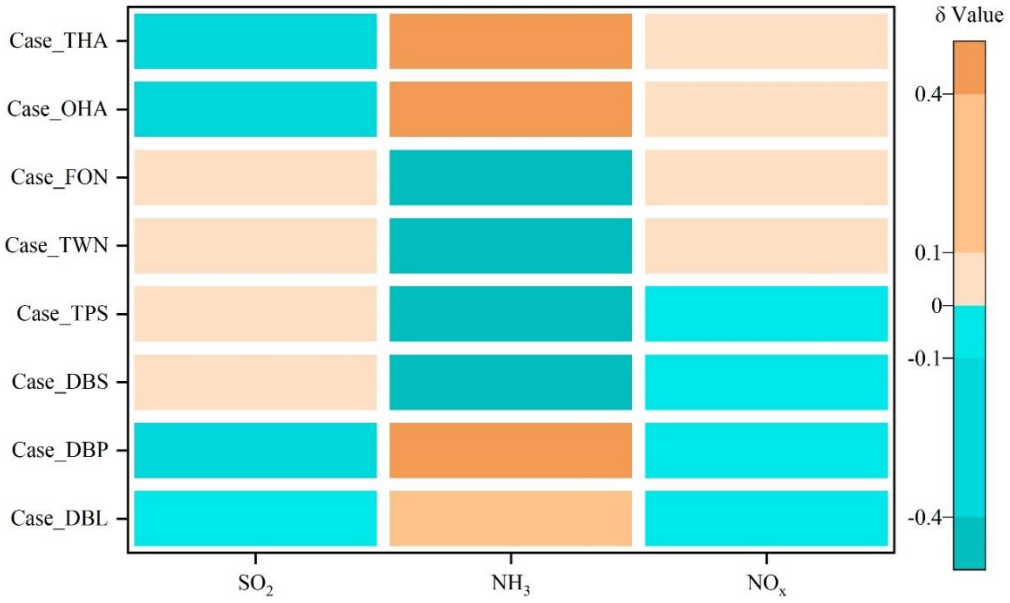

Fig.9 The sensitivity coefficients (δ) of simulated gas pollutants to the change of adopted source profile in different cases.

Similarly, with the increase of metal ions in the system to bond with anions, the number of anions which can bind to NH_4^+ decreased. The system needed less NH_4^+ and weakened the need for conversion from NH_3 to NH_4^+, the simulated NH_4^+ concentration decreased while the δ of NH_3 was positive and very sensitive. Different trends of simulated concentration of gaseous pollutants mirrored the rules mentioned above from another aspect. The δ of SO_2 and NO_x was negative, NH_3 was positive. We could see the same phenomena in DBL case (Fig. 9). When the percentages of Non-SNA in source profile increased, they not only affected the simulated concentration of Non-SNA, but also the secondary SO_4^{2-}, NO_3^- and NH_4^+.

In SO_4^{2-} perturbation cases (Case DBS and TPS), as the percentage of SO_4^{2-} in

source profile increased, for the chemical reactions of sulfate radical consuming (as shown in Table S22), the chemical equilibrium would move toward the products when compared to the base case. While for the chemical reactions of sulfate radical formation (The equations were shown in Table S23), meant the product was added in, the chemical equilibrium would be pushed toward the reactants. The chemical reactions between SO_4^{2-} and NH_4^+ would shift to the direction of $(NH_4)_2SO_4$ generation, we could see the simulated concentrations of NH_4^+ in DBS and TPS were both higher and NH_3 were lower than those in the base case (SGL). In addition, when more SO_4^{2-} was added in, the conversion of SO_2 to SO_4^{2-} was affected in some level and consumed less SO_2 than the base case, simulated SO_2 showed insensitive but positive trend (Fig.9). And from the potential solid phase species in ISORROPIA II under DBS and TPS cases (Table 3), the solid phase species were mainly consisted of sulfate salts, so the simulated concentration of NO_3^- did not change apparently.

As the percentage of NO_3^- in source profile increased (Case FON and TWN), the associated chemical equilibrium shifted towards the consumption of NO_3^-, such as $NH_4^+ + NO_3^- \rightarrow NH_4NO_3$, which would also consume more NH_4^+ and form more ammonium salt, finally consumed more NH_3 because of $NH_3(gas) + H_2O(aq) \rightarrow NH_4^+(aq) + OH^-(aq)$. The simulation results also manifested that the concentration of NH_4^+ increased while that of NH_3 decreased. Based on the assumption of ISORROPIA, the cations like Na^+, K^+, Mg^{2+}, Ca^{2+} and NH_4^+ preferentially to react with SO_4^{2-}, only if there were cations left after neutralized SO_4^{2-}, could they react with NO_3^- to form salts, so the simulated concentration of SO_4^{2-} was not obviously changed. Accordingly, the simulated concentration of NO_x and SO_2 almost unchanged (The δ of NO_x and SO_2 was insensitive).

In the cases of NH_4^+ perturbation (Case OHA and THA), when the percentage of NH_4^+ in source profile increased, the related chemical equilibrium shifted towards the direction of NH_4^+ consumption, such as in $2NH_4^+ + SO_4^{2-} \rightarrow (NH_4)_2SO_4$, more SO_4^{2-} was consumed at the same time, which further promoted the conversion of SO_2 to SO_4^{2-}. The increased NH_4^+ in OHA and THA also would inhibit the conversion of NH_3 to NH_4^+

when compared to the base case. This, in turn appeared as the increase of the simulated secondary SO_4^{2-} and NH_3, and the decrease of the simulated SO_2.

In summary, the effects of source profile variation on the simulation results of different components were linked. When the percentages of Non-SNA, SO_4^{2-}, NO_3^- and NH_4^+ in the source profile changed, they not only affected the simulated concentration of themselves, but also affected the simulation results of some other components. Both the simulation results of primary components and secondary components were affected by the change of source profile, the secondary SO_4^{2-} and NH_4^+ were affected more than the secondary NO_3^-.

6 Conclusions

Although the influence of source profile variation on the simulated concentration of ambient $PM_{2.5}$ is not significant, its influence on the simulated chemical components cannot be ignored. The variation of simulated components ranges from 8% to 167% under selected different source profiles, and the simulation results of some components are sensitive to the adopted $PM_{2.5}$ source profile in CTMs, e.g., both the simulated Non-SNA and SNA are sensitive to the perturbation of Non-SNA in source profile, the simulated SO_4^{2-} and NH_4^+ are sensitive to the perturbation of SO_4^{2-}, simulated NO_3^- and NH_4^+ are sensitive to the perturbation of NO_3^-, SO_4^{2-} and NH_4^+ are sensitive to the perturbation of NH_4^+. These influences are not only specific to an individual component, but also can be transmitted and linked among components, that is, the influence path is connected to chemical mechanisms in the model since the variation of species allocation in emission sources directly affect the thermodynamic equilibrium system (ISORROPIA II, SO_4^{2-}-NO_3^--Cl^--NH_4^+-Na^+-K^+-Mg^{2+}-Ca^{2+}-H_2O system).

Traditionally, the source profiles are regarded as a primary emission, but interestingly, their variation could affect the simulation result of secondary components as well in CTMs. We found the perturbation of $PM_{2.5}$ source profile caused the variation of simulated gaseous pollutants, and related chemical reactions like gas-phase chemistry of SO_2, NO_x and NH_3, which mirrored that the perturbation of source profile

had an effect on the simulation of secondary $PM_{2.5}$ components. Overall, the emission source profile used in CTMs is one of the important factors affecting the simulation results of $PM_{2.5}$ chemical components. Additionally, organic species are one of the most important components in $PM_{2.5}$ and gain much more attention on human health. While the number of organic species in source profile is relatively scarce which brings a challenge for simulation test designing, the variation of source profile adopted in CTMs has an impact on the simulation of organic species is not taken into account in this study.

With the change of fuel and raw materials, the development of production technology and the innovation of pollution treatment technology in recent years, some components have changed significantly in the source profile. Given the important role of air quality simulation in environment management and health risk assessment, the representativeness and timeliness of the source profile should be considered.

Our study tentatively discussed the impact mechanism of emission source profiles on $PM_{2.5}$ components simulation results in CTMs. In the next work, we will use different source profile for simulation, compare the simulation results with local measured $PM_{2.5}$ components and discuss the influence of sub-source profiles variation on the simulation results. In addition, the size distribution, mixing state, aging and solubility for different aerosol components might have something to do with source profile, how much the influence of source profile changes on these physical and chemical process, is deserved to do in the future.

Data availability

The input datasets for WRF simulation are available at https://rda.ucar.edu/datasets/ds351.0/index.html (The National Center for Atmospheric Research (NCAR)). The Multi-resolution Emission Inventory for China (MEICv1.3) is available at http://meicmodel.org/?page_id=135. The $PM_{2.5}$ emission source profiles from database of Source Profiles of Air Pollution (SPAP) (http://www.nkspap.com:9091/, Nankai university), SPECIATE database (https://www.epa.gov/air-emissions-modeling/speciate, U.S. Environmental Protection

Agency's (EPA)), Mendeley data repository (https://doi.org/10.17632/x8dfshjt9j.2, Bi et al., 2019).

Code availability

The source code for CMAQ version 5.0.2 is available at https://github.com/USEPA/CMAQ/tree/5.0.2 (last access: April 2014) (https://doi.org/10.5281/zenodo.1079898, US EPA Office of Research and Development, 2018). The source code for WRF version 3.7.1 is available at ~~https://github.com/NCAR/WRFV3 (last access: 14 August 2015, NCAR)~~ https://www2.mmm.ucar.edu/wrf/src/WRFV3.7.1.TAR.gz.

Author contributions

Zhongwei Luo: Data curation and collection, writing–original draft. Yan Han: Modeling, writing–original draft. Kun Hua: Data collection. Yufen Zhang: Supervision–Review & editing. Jianhui Wu: Supervision in source profile. Xiaohui Bi: Supervision in source profile. Qili Dai: Resources. Baoshuang Liu: Resources. Yang Chen: Modification and editing. Xin Long: Supervision in modeling. Yinchang Feng: Supervision–Review & editing.

Competing interests

The authors declare that they have no known competing financial interests or personal relationships that could have appeared to influence the work reported in this paper.

Disclaimer. Publisher's note

Copernicus Publications remains neutral with regard to jurisdictional claims in published maps and institutional affiliations.

Acknowledgements

We would like to thank the National Natural Science Foundation of China (grant number 42177465) for providing funding for the project. We are grateful for the

Inventory Spatial Allocate Tool (ISAT) provided by Kun Wang from Department of Air Pollution Control, Institute of Urban Safety and Environmental Science, Beijing Academy of Science and Technology. We thank two anonymous referees and Astrid Kerkweg (Executive Editor) for helpful discussion.

Financial support

This study was financially supported by the National Natural Science Foundation of China (grant number 42177465).

Reference

Appel, K. W., Poulio, G. A., Simon, H., Sarwar, G., Pye, H. O. T., Napelenok, S. L., Akhtar, F., Roselle, S. J.: Evaluation of dust and trace metal estimates from the Community Multiscale Air Quality (CMAQ) model version 5.0, Geosci. Model Dev., 6, 883-899, https://doi.org/10.5194/gmd-6-883-2013, 2013.

Bi, X., Dai, Q., Wu, J., Zhang, Q., Zhang, W., Luo, R., Cheng, Y., Zhang, J., Wang, L., Yu, Z., Zhang, Y., Tian, Y., Feng, Y.: Characteristics of the main primary source profiles of particulate matter across China from 1987 to 2017, Atmos. Chem. Phys., 19, 3223-3243, https://doi.org/10.5194/acp-19-3223-2019, 2019.

Cao, J., Qiu, X., Gao, J., Wang, F., Wang, J., Wu, J., Peng, L.: Significant decrease in SO_2 emission and enhanced atmospheric oxidation trigger changes in sulfate formation pathways in China during 2008–2016, J. Clean. Prod., 326, 129396, https://doi.org/10.1016/j.jclepro.2021.129396, 2021.

Chapel Hill, N.: Operational Guidance for the Community Multiscale Air Quality (CMAQ) Mo deling System Version 5.0, https://www.airqualitymodeling.org/index.php/CMAQ_version_5.0_(February_2010_release)_OGD#Aerosol_Module, last access: February 2012.

Chen, Z., Chen, D., Zhao, C., Kwan, M., Cai, J., Zhuang, Y., Zhao, B., Wang, X., Chen, B., Yang, J., Li, R., He, B., Gao, B., Wang, K., Xu, B.: Influence of meteorological conditions on $PM_{2.5}$ concentrations across China: A review of methodology and mechanism, Environ. Int., 139, 105558, https://doi.org/10.1016/j.envint.2020.105558, 2020.

Cheng, N. L., Meng, F., Wang, J. K., Chen, Y. B., Wei, X., Han, H.: Numerical simulation of the spatial distribution and deposition of $PM_{2.5}$ in East China coastal area in 2010 (In Chinese), Journ. Safety Environ., 15, 305-310, https://doi.org/10.13637/j.issn.1009-6094.2015.06.063, 2015.

Foley, K. M., Roselle, S. J., Appel, K. W., Bhave, P. V., Pleim, J., Otte, T., Mathur, R., Sarwar, G., Young, J. O., Gilliam, R.: Incremental testing of the community multiscale air quality (CMAQ) modeling system version 4.7, Geosci. Model Dev., 3, 205-226, https://doi.org/10.5194/gmd-3-205-2010, 2010.

Fountoukis, C., Nenes, A.: ISORROPIA II: a computationally efficient thermodynamic equilibrium model for K^+–Ca^{2+}–Mg^{2+}–NH_4^+–Na^+–SO_4^{2-}–NO_3^-–Cl^-–H_2O aerosols, Atmos. Chem. Phys., 7, 4639-4659, https://doi.org/10.5194/acp-7-4639-2007, 2007.

Fu, X., Wang, S., Zhao, B., Xing, J., Cheng, Z., Liu, H., Hao, J.: Emission inventory of primary pollutants and chemical speciation in 2010 for the Yangtze River Delta region, China, Atmos. Environ., 70, 39-50, https://doi.org/10.1016/j.atmosenv.2012.12.034, 2013.

Fu, X., Wang, S. X., Chang, X., Cai, S., Xing, J., Hao, J. M.: Modeling analysis of secondary inorganic aerosols over China: pollution characteristics, and meteorological and dust impacts, Sci. Rep., 6, 35992, https://doi.org/10.1038/srep35992, 2016.

Gao, S., Zhang, S., Che, X., Ma, Y., Chen, X., Duan, Y., Fu, Q., Wang, S., Zhou, B., Wei, C., Jiao, Z.: New understanding of source profiles: Example of the coating industry, J. Clean. Prod., 357, 132025, https://doi.org/10.1016/j.jclepro.2022.132025, 2022.

Guo, R., Yang, J., Liu, Z.: Influence of heat treatment conditions on release of chlorine from Datong coal, J. Anal. Appl. Pyrol., 71, 179-186, https://doi.org/10.1016/S0165-2370(03)00086-X, 2004.

Guo, Y. Y., Gao, X., Zhu, T. Y., Luo, L., Zheng, Y.: Chemical profiles of PM emitted from the iron and steel industry in northern China, Atmos. Environ., 150, 187-197, https://doi.org/10.1016/j.atmosenv.2016.11.055, 2017.

Guo, Z., Hao, Y., Tian, H., Bai, X., Wu, B., Liu, S., Luo, L., Liu, W., Zhao, S., Lin, S., Lv, Y., Yang, J., Xiao, Y.: Field measurements on emission characteristics, chemical profiles, and emission factors of size-segregated PM from cement plants in China, Sci. Total Environ., 151822, https://doi.org/10.1016/j.scitotenv.2021.151822, 2021.

Han, Y., Xu, H., Bi, X. H., Lin, F. M., Li, J., Zhang, Y. F., Feng, Y. C.: The effect of atmospheric particulates on the rainwater chemistry in the Yangtze River Delta, China, J. Air Waste Manage., 69, 1452-1466, https://doi.org/10.1080/10962247.2019.1674750, 2019.

Hopke, P. K., Dai, Q., Li, L., Feng, Y.: Global review of recent source apportionments for airborne particulate matter, Sci. Total Environ., 740, 140091, https://doi.org/10.1016/j.scitotenv.2020.140091, 2020.

Hopke, P. K., Feng, Y. C., Dai, Q.: Source apportionment of particle number concentrations: A global review, Sci. Total Environ., 819, 153104, https://doi.org/10.1016/j.scitotenv.2022.153104, 2022.

Hsu, Y., Divita, F., Dorn, J.: SPECIATE 5.0 - Speciation Database Development Documentation, Final Report, M. MENETREZ, Abt Associates Inc./Office of Research and Development/U.S. Environmental Protection Agency Research Triangle Park, NC27711, https://www.epa.gov/sites/default/files/2019-07/documents/speciate_5.0.pdf, 2019.

Huang, C. H., Hu, J. L., Xue, T., Xu, H., Wang, M.: High-Resolution Spatiotemporal Modeling for Ambient $PM_{2.5}$ Exposure Assessment in China from 2013 to 2019, Environ. Sci. Technol., 55, 2152-2162, https://doi.org/10.1021/acs.est.0c05815, 2021.

Huang, Z. J., Zheng, J. Y., Qu, J. M., Zhong, Z. M., Wu, Y. Q., Shao, M.: A Feasible Methodological Framework for Uncertainty Analysis and Diagnosis of Atmospheric Chemical Transport Models, Environ. Sci. Technol., 53, 3110-3118, https://doi.org/10.1021/acs.est.8b06326, 2019.

Ji, Z., Gan, M., Fan, X., Chen, X., Li, Q., Lv, W., Tian, Y., Zhou, Y., Jiang, T.: Characteristics of $PM_{2.5}$ from iron ore sintering process: Influences of raw materials and controlling methods, J. Clean. Prod., 148, 12-22, https://doi.org/10.1016/j.jclepro.2017.01.103, 2017.

Li, J., Wu, Y., Ren, L., Wang, W., Tao, J., Gao, Y., Li, G., Yang, X., Han, Z., Zhang, R.: Variation in $PM_{2.5}$ sources in central North China Plain during 2017–2019: Response to mitigation strategies, J. Environ. Manage., 28, 112370, https://doi.org/10.1016/j.jenvman.2021.112370, 2021.

Li, M., Hu, M., Du, B., Guo, Q., Tan, T., Zheng, J., Huang, X., He, L., Wu, Z., Guo, S.: Temporal and spatial distribution of $PM_{2.5}$ chemical composition in a coastal city of Southeast China, Sci. Total Environ., 605-606, 337-346, https://doi.org/10.1016/j.scitotenv.2017.03.260, 2017a.

Li, M., Liu, H., Geng, G., Hong, C., Liu, F., Song, Y., Tong, D., Zheng, B., Cui, H., Man, H., Zhang, Q., He, K.: Anthropogenic emission inventories in China: a review, Natl. Sci. Rev., 4, 834-866,

https://doi.org/10.1093/nsr/nwy044, 2017b.
Li, X., He, K., Li, C., Yang, F., Zhao, Q., Ma, Y., Chen, Y., Ouyang, W., Chen, G.: $PM_{2.5}$ mass, chemical composition, and light extinction before and during the 2008 Beijing Olympics, J. Geophys. Res., 118, 12158-12167, https://doi.org/10.1002/2013JD020106, 2013.
Liang, F., Xiao, Q., Yang, X., Liu, F., Li, J., Lu, X., Liu, Y., Gu, D.: The 17-y spatiotemporal trend of $PM_{2.5}$ and its mortality burden in China, Proc. Natl. Acad. Sci., 117, 25601-25608, https://doi.org/10.1073/pnas.1919641117, 2020.
Lv, L., Wei, P., Li, J., Hu, J.: Application of machine learning algorithms to improve numerical simulation prediction of $PM_{2.5}$ and chemical components, Atmos. Pollut. Res., 12, 101211, 10.1016/j.apr.2021.101211, 2021.
NBS (National Bureau of Statistics of China): China Statistical Yearbook 2021, http://www.stats.gov.cn/tjsj/ndsj/2021/indexch.htm, last access: 2022.
Peterson, G., Hogrefe, C., Corrigan, A., Neas, L., Mathur, R., Rappold, A.: Impact of Reductions in Emissions from Major Source Sectors on Fine Particulate Matter–Related Cardiovascular Mortality, Environ, Health Persp., 128, 017005, https://doi.org/10.1289/EHP5692, 2020.
Qi, H., Cui, C., Zhao, T., Bai, Y., Liu, L.: Numerical simulation on the characteristics of $PM_{2.5}$ heavy pollution and the influence of weather system in Hubei Province in winter 2015 (In Chinese), Meteorological monthly, 45, 1113-1122, https://doi.org/10.7519/j.issn.1000-0526.2019.08.008, 2019.
Seinfeld, J. H., Pandis, S. N.: Atmospheric Chemistry and Physics, from air pollution to climate change. John Wiley & Sons, Inc., Hoboken, New Jersey.47-61, ISBN9781119221166, 2006
Sha, T., Ma, X., Jia, H., Tian, R., Chang, Y., Cao, F., Zhang, Y.: Aerosol chemical component: Simulations with WRF-Chem and comparison with observations in Nanjing, Atmos. Environ., 218, 1-14, https://doi.org/10.1016/j.atmosenv.2019.116982, 2019.
Shi, W., Liu, C., Norback, D., Deng, Q., Huang, C., Qian, H., Zhang, X., Sundell, J., Zhang, Y., Li, B., Kan, H., Zhao, Z.: Effects of fine particulate matter and its constituents on childhood pneumonia: a cross-sectional study in six Chinese cities, Lancet, 392, S79, https://doi.org/10.1016/S0140-6736(18)32708-9, 2018.
Shi, Z., Li, J., Huang, L., Wang, P., Wu, L., Ying, Q., Zhang, H., Lu, L., Liu, X., Liao, H., Hu, J.: Source apportionment of fine particulate matter in China in 2013 using a source-oriented chemical transport model, Sci. Total Environ., 601-602, 1476-1487, https://doi.org/10.1016/j.scitotenv.2017.06.019, 2017.
Song, S. Y., Wang, Y. S., Wang, Y. L., Wang, T., Tan, H. Z.: The characteristics of particulate matter and optical properties of Brown carbon in air lean condition related to residential coal combustion, Powder Technol., 379, 505-514, https://doi.org/10.1016/j.powtec.2020.10.082, 2021.
Tang, X. Y., Zhang, Y. H., Shao, M.: Atmosphere Environment Chemistry, Second ed (In Chinese). . Higher Education Press, Beijing, China.268-329, ISBN978-7-04-019361-9, 2006
Wang, C., Zheng, J., Du, J., Wang, G., Klemes, J., Wang, B., Liao, Q., Liang, Y.: Weather condition-based hybrid models for multiple air pollutants forecasting and minimisation, J. Clean. Prod., 352, 131610, https://doi.org/10.1016/j.jclepro.2022.131610, 2022.
Wang, D., Hu, J., Xu, Y., Lv, D., Xie, X., Kleeman, M., Xing, J., Zhang, H., Ying, Q.: Source contributions to primary and secondary inorganic particulate matter during a severe wintertime $PM_{2.5}$ pollution episode in Xi'an, China, Atmos. Environ., 97, 182-194, https://doi.org/10.1016/j.atmosenv.2014.08.020, 2014.

729 Weagle, C., Sinder, G., Li, C. C., Donkelaar, A., S, P., Bissonnette, P., Burke, I., Jackson, J., Latimer, R.,
730 Stone, E., Abboud, I., Akoshile, C., Anh, N., Brook, J., Cohen, A., Dong, J., Gibson, M., Griffith,
731 D., He, K., Holben, B., Kahn, R., Keller, C., Kim, J., Lagrosas, N., Lestari, P., Khian, Y., Liu, Y.,
732 Marais, E., Martins, J., Misra, A., Muliane, U., Pratiwi, R., Quel, E., Salam, A., Segey, L., Tripathi,
733 S., Wang, C., Zhang, Q., Brauer, M., Rudich, Y., Martin, R.: Global Sources of Fine Particulate
734 Matter: Interpretation of $PM_{2.5}$ Chemical Composition Observed by SPARTAN using a Global
735 Chemical Transport Model, Environ. Sci. Technol., 52, 11670-11681,
736 https://doi.org/10.1021/acs.est.8b01658, 2018.
737 Wongphatarakul, V., Friedlander, S. K., Pinto, J. P.: A Comparative Study of $PM_{2.5}$ Ambient Aerosol
738 Chemical Databases, Environ. Sci. Technol., 32, 3926-3934, https://doi.org/10.1021/es9800582,
739 1998.
740 Wu, B., Bai, X., Liu, W., Zhu, C., Hao, Y., Lin, S., Liu, S., Luo, L., Liu, X., Zhao, S., Hao, J., Tian, H.:
741 Variation characteristics of final size-segregated PM emissions from ultralow emission coal-fired
742 power plants in China, Environ. Pollut., 259, 113886, https://doi.org/10.1016/j.envpol.2019.113886,
743 2020.
744 Wu, D., Zheng, H., Li, Q., Jin, L., Lyu, R., Ding, X., Huo, Y., Zhao, B., Jiang, J., Chen, J., Li, X., Wang,
745 S.: Toxic potency-adjusted control of air pollution for solid fuel combustion, Nat. Energy, 7, 194-
746 202, https://doi.org/10.1038/s41560-021-00951-1, 2022.
747 Wu, Z. X., Hu, T. F., Hu, W., Shao, L. Y., Sun, Y. Z., Xue, F. L., Niu, H. Y.: Evolution in physicochemical
748 properties of fine particles emitted from residential coal combustion based on chamber experiment,
749 Gondwana Res., https://doi.org/10.1016/j.gr.2021.10.017, 2021.
750 Xia, Z. Q., Fan, X. L., Huang, Z. J., Liu, Y. C., Yin, X. H., Ye, X., Zheng, J. Y.: Comparison of Domestic
751 and Foreign $PM_{2.5}$ Source Profiles and Influence on Air Quality Simulation (In Chinese), Res.
752 Environ. Sci., 30, 359-367, https://doi.org/10.13198/j.issn.1001-6929.2017.01.55, 2017.
753 Yang, F., Tan, J., Zhao, Q., Du, Z., He, K., Ma, Y., Duan, F., Chen, G., Zhao, Q.: Characteristics of $PM_{2.5}$
754 speciation in representative megacities and across China, Atmos. Chem. Phys., 11, 1025-1051,
755 https://doi.org/10.5194/acpd-11-1025-2011, 2011.
756 Ying, Q., Feng, M., Song, D. L., Wu, L., Hu, J., Zhang, H., Kleeman, M., Li, X.: Improve regional
757 distribution and source apportionment of $PM_{2.5}$ trace elements in China using inventory-observation
758 constrained emission factors, Sci. Total Environ., 624, 355-365,
759 https://doi.org/10.1016/j.scitotenv.2017.12.138, 2018.
760 Yu, Z. C., Jang, M., Kim, S., Bae, C., Koo, B., Beardsley, R., Park, J., Chang, L., Lee, H., Lim, Y., Cho,
761 J.: Simulating the Impact of Long-Range-Transported Asian Mineral Dust on the Formation of
762 Sulfate and Nitrate during the KORUS-AQ Campaign, Earth Space Chem., 4, 1039-1049,
763 https://doi.org/10.1021/acsearthspacechem.0c00074, 2020.
764 Zhang, J., Wu, J., Lv, R., Song, D., Huang, F., Zhang, Y., Feng, Y.: Influence of Typical Desulfurization
765 Process on Flue Gas Particulate Matter of Coal-fired Boilers (In Chinese), Environ. Sci., 41, 4455-
766 4461, https://doi.org/10.13227/j.hjkx.202003193, 2020.
767 Zhang, Q., Xue, D., Wang, S., Wang, L., Wang, J., Ma, Y., Liu, X.: Analysis on the evolution of $PM_{2.5}$
768 heavy air pollution process in Qingdao (In Chinese), China Environ. Sci., 37, 3623-3635,
769 https://doi.org/10.3969/j.issn.1000-6923.2017.10.003, 2017.
770 Zhang, S. P., Xing, J., Sarwar, G., Ge, Y. L., He, H., Duan, F., Zhao, Y., He, K., Zhu, L., Chu, B.:
771 Parameterization of heterogeneous reaction of SO_2 to sulfate on dust with coexistence of NH_3 and
772 NO_2 under different humidity conditions, Atmos. Environ., 208, 133-140,

https://doi.org/10.1016/j.atmosenv.2019.04.004, 2019.

Zheng, B., Tong, D., Li, M., Liu, F., Hong, C., Geng, G., Li, H., Li, X., Peng, L., Qi, J., Yan, L., Zhang, Y., Zhao, H., Zheng, Y., He, K., Zhang, Q.: Trends in China's anthropogenic emissions since 2010 as the consequence of clean air actions, Atmos. Chem. Phys., 18, 14095-14111, https://doi.org/10.5194/acp-18-14095-2018, 2018.

Zheng, B., Zhang, Q., Zhang, Y., He, K. B., Wang, K., Zheng, G. J., Duan, F. K., Ma, Y. L., Kimoto, T.: Heterogeneous chemistry: a mechanism missing in current models to explain secondary inorganic aerosol formation during the January 2013 haze episode in North China, Atmos. Chem. Phys., 15, 2031–2049, https://doi.org/10.5194/acp-15-2031-2015, 2015.

Zheng, H., Song, S., Sarwar, G., Gen, M., Wang, S., Ding, D., Chang, X., Zhang, S., Xing, J., Sun, Y. L., Ji, D., Chan, C. K., Gao, J., Mcelory, M.: Contribution of Particulate Nitrate Photolysis to Heterogeneous Sulfate Formation for Winter Haze in China, Environ. Sci. Technol. Lett., 7, 632-638, https://doi.org/10.1021/acs.estlett.0c00368, 2020.

Zhou, L., Chen, X., Tian, X.: The impact of fine particulate matter ($PM_{2.5}$) on China's agricultural production from 2001 to 2010, J. Clean. Prod., 178, 133-141, https://doi.org/10.1016/j.jclepro.2017.12.204, 2018.